Interface Electronic Structure by the Renormalization Method: Theory and Application to Sb/GaAs

A. Bödicker and W. Schattke
Institut für Theoretische Physik
Universität Kiel
D-24118 Kiel, Federal Republic of Germany

J. Henk and R. Feder
Theoretische Festkörperphysik – FB 10
Universität Duisburg – GH
D-47048 Duisburg, Federal Republic of Germany

Figures are incomplete.

short title: **Interface Electronic Structure of Sb/GaAs**

PACS numbers: 73.20.At, 71.20.Ad, 71.25.Cx

Abstract

In this paper we present a highly convergent renormalization scheme for the computation of Green's functions of interfaces in the case of tight-binding models. It allows the calculation of the Green's function of the whole infinite system, which is built by a stack of a semi-infinite solid of material A, an interface region, and of a semi-infinite solid of material B. As a first application we analyse the layer-resolved interface electronic structure of Sb/GaAs(110) and compare the results with calculations for (xML)Sb/GaAs(110), $x = 1$, 2, and 3. We find several interface states in the fundamental band gap of GaAs(110). Their energy dispersion and orbital composition are discussed in detail. Furthermore, we find that the interface electronic structure of (3ML)Sb/GaAs(110) still differs significantly from that of the system terminated by a semi-infinite Sb crystal.

1 Introduction

The key to calculations of the electronic structure of solids is the Green's function. It allows the determination of electronic properties, such as the layer density of states (LDOS) or the charge density, and may be used also in cases where the threedimensional periodicity of the system is destroyed, as *e. g.* for surface-terminated solids, for solids containing defects, for interfaces, and for superlattices.

A lot of computational schemes for the determination of the Green's function of interfaces have been developed, especially in the case of tight-binding models. Schulman and Chang (1983) introduced a so-called reduced Hamiltonian method. At the interface, transfer matrices are used for the determination of the total wave function, which itself is expanded into bulk states with complex wave vector far away from the interface. Lambrecht and Andersen (1986) developed a scheme for tight-binding muffin-tin orbitals based on the Green's function matrix of the ideal system. In recent publications Skriver and Rosengaard (1992; Rosengaard and Skriver 1993) applied this method to the surface and interface electronic structure within a comprehensive implementation. The method of Green's function matching has been applied to surfaces and interfaces by Muñoz *et al* (1987). Furthermore, a difference-equation approach has been developed by Chen *et al* (1989). A renormalization formalism for the calculation of the electronic structure of superlattices has been deduced by Graft *et al* (1987) and applied to silicon superlattices. The Green's function of solids with bulk- or surface-located defects has been derived by Wachutka *et al* (1992). A survey of several methods is given by Grosso *et al* (1989). At last, we have to mention an approach based on multiple scattering theory by MacLaren *et al* (1989).

In a previous publication we have formulated a renormalization procedure based on the work of Lopéz Sancho *et al* (1985), which allows a fast computation of surface electronic properties in the case of tight-binding models (Henk and Schattke 1993a). In this paper we present an extension of this calculational scheme to interfaces and discuss in detail the electronic properties of the Sb/GaAs interface.

The renormalization method described here allows a highly efficient numerical implementation. Furthermore, the in principle infinite number of iteration steps can be significantly reduced by well-defined break conditions which yield a controlled error in the results. For example, in practical calculations not more than 10 iterations are necessary to reduce the error in the LDOS due to the termination of the renormalization loop below 1 per cent. Via transfer matrices the complete Green's function matrix of the stack of the two semi-infinite solids can be easily computed. This allows a detailed analysis of the hybridization of resonances with bulk states and of the decay of interface-state wave functions in direction normal to the interface plane. Due to the high efficiency of the method and to the simplicity of the underlying tight-binding formalism large unit cells as well as large basis sets can be treated.

In the last years there has been growing interest in systems with many adsorbed layers. The experimental and theoretical study of the geometrical and electronic structure of layer-by-layer grown adsorbates allows an analysis of the transition from the monolayer to the bulk crystal. At the interface, *i. e.* the boundary between the substrate and the adsorbate, the localized states will be considerably influenced by the boundary condition at the surface side of the system, especially if the number of adsorbed layers is rather small.

In calculations of the electronic structure of surfaces applying sophisticated computation schemes, the semi-infinite system is often represented by a slab of few atomic layers (see for example Hybertsen and Louie 1987, Kress *et al* 1993). An extension of this approach to treat an interface is rather difficult due to the small number of layers associated with the two materials. At first, an increase of the slab size will raise the computation time considerably. Second, the electron states located at the interface may be perturbed by 'wrong' boundary conditions at the two surfaces of the slab. This may happen for example if the interface states overlap with the surface states, leading to erroneous results. In other words, interface region and surface have to decouple to yield a reliable interface electronic structure. Here, the need for a computational scheme taking into account the stacking of two semi-infinite solids appears. Nevertheless, slab methods in their linear versions yield all energy eigenvalues at once by a single inversion of the (large) Hamiltonian matrix, whereas in Green function methods the energy has to be scanned but smaller matrices have to be inverted.

In the past decades Schottky barriers have attracted constant interest in the solid state field and a lot of empirical data have been accumulated (for a review see Mönch 1986) with an apparent need for theoretical calculations on a microscopic basis. Therefore, such an interface lends itself support as a first application of the calculational scheme presented below. We choose the Sb/GaAs interface because the adsorbate system (1ML)Sb/GaAs(110) has been studied both experimentally and theoretically. The geometrical structure has been determined by LEED (low-energy electron diffraction) (Duke *et al* 1982) and LEPD (low-energy positron diffraction) (Chen *et al* 1993), whereas the electronic structure has been analysed both theoretically (Bertoni *et al* 1983) and by angle-resolved photoemission spectroscopy experimentally (Mårtensson *et al* 1986). Our main interest is to analyse the difference in the interface electronic structure of surface-terminated systems such as (xML)Sb/GaAs, $x = 1$, 2, and 3, with respect to the interface electronic structure of the system terminated by a semi-infinite Sb-crystal. Because the lattice constants of both GaAs and Sb differ incommensurably we introduce so-called averaged tight-binding parameters. This is necessary because translational invariance parallel to the interface layer is an essential ingredient in a layer-renormalization scheme.

The renormalization method has also been applied to the Co/Cu interface successfully (Reiser 1993). A detailed analysis of the rich spin-resolved interface-band structure will be published elsewhere.

2 Theory

In this section we give a short description of the renormalization procedure for the interface electronic structure. Because it is an extension of the method used for the computation of the surface electronic structure only new features will be presented in detail. Therefore, we refer to a previous publication (Henk and Schattke 1993a).

2.1 Layer Bloch sums and interaction matrices

As basis we choose Bloch sums

$$\langle \vec{r} \mid n\alpha \rangle = \frac{1}{\sqrt{N_{\|}}} \sum_j \exp[i\vec{k}_{\|} \cdot (\vec{R}_j + \vec{r}_\alpha)] \; \Phi_\alpha(\vec{r} - \vec{R}_j - \vec{r}_\alpha) \qquad (1)$$

which are labelled by the layer index n. All other state characteristics, for example the atomic quantum numbers, are condensed into one multi-index α. Here, Φ_α

denotes an atomic orbital. The sum runs over all $N_{||}$ unit cells of layer n. In the considerations below, we take the component $\vec{k}_{||}$ of the wave vector as fixed and, therefore, suppress it.

The solid we are concerned with may be seen as a stack consisting of a semi-infinite crystal of material A, the interface region I, and a semi-infinite solid of material B. Furthermore, translational symmetry parallel to the interface is assumed.

As a next step we introduce so-called *principal layers*, *i. e.*, a stack of atomic layers, such that only Bloch sums localized at adjacent principal layers interact. The numbers of Bloch sums per principal layer in the three regions are denoted N_{A}, N_{I}, and N_{B}, respectively. Furthermore, we chose the interface region as being built by a single principal layer with layer index set arbitrarily to 0. Material A consists of principal layers with positive index n, material B of those with negative index n.

Due to this arrangement the interaction between Bloch sums in the region filled by material A is described by $N_{\mathrm{A}} \times N_{\mathrm{A}}$-matrices which will be abbreviated as follows (confer Henk and Schattke 1993a):

$$A_{00} = z\, S_{nn} - H_{nn}, \tag{2a}$$

$$-A_{01} = z\, S_{n,n+1} - H_{n,n+1}, \tag{2b}$$

$$-A_{01}^{\dagger} = z\, S_{n+1,n} - H_{n+1,n} \tag{2c}$$

for $n \geq 1$, n being the principal layer index. Here, z denotes the complex energy, $z = E + i\eta, \eta \geq 0$. S and H are the overlap and the Hamiltonian matrices. The interaction in material B is described in a similar way by $N_{\mathrm{B}} \times N_{\mathrm{B}}$-matrices,

$$B_{00} = z\, S_{nn} - H_{nn}, \tag{3a}$$

$$-B_{01} = z\, S_{n-1,n} - H_{n-1,n}, \tag{3b}$$

$$-B_{01}^{\dagger} = z\, S_{n,n-1} - H_{n,n-1} \tag{3c}$$

for $n \leq -1$. The intralayer interaction of the interface principal layer is given by the $N_{\mathrm{I}} \times N_{\mathrm{I}}$-matrix

$$I_{00} = z\, S_{00} - H_{00}. \tag{4}$$

Due to the *nearest neighbour coupling* of principal layers Bloch sums of region A do not interact directly with those of region B. The interaction of the material A region to the interface layer is described by a $N_{\mathrm{I}} \times N_{\mathrm{A}}$- and a $N_{\mathrm{A}} \times N_{\mathrm{I}}$-matrix:

$$-A_{01}^{\mathrm{s}} = z\, S_{01} - H_{01}, \tag{5a}$$

$$-A_{01}^{s\dagger} = z\ S_{10} - H_{10}. \tag{5b}$$

In the same way we arrive at

$$-B_{01}^{s} = z\ S_{-1,0} - H_{-1,0}, \tag{6a}$$

$$-B_{01}^{s\dagger} = z\ S_{0,-1} - H_{0,-1}. \tag{6b}$$

for the coupling of material B to the interface layer. A matrix labelled with a dagger ($\dagger$) is in general not the hermitian conjugate of the respective matrix without dagger because z may be complex.

Because our basis set may be nonorthogonal, *i. e.* S may be not equal to the unit matrix, the Green's function is given in a conjugate basis (Ballentine and Kolář 1986). In this paper we omit the distinction of the two basis sets because it should be clear which basis is currently used.

2.2 Renormalization instructions

Due to the renormalization method one eliminates block matrices of the Green's function with odd principal-layer index. Observing that the resulting equations possess the same structure as the starting equations the same elimination procedure could be carried out. This leads to a set of renormalization instructions which in our case read

$$I_{00} \to I_{00} - B_{01}^{s\dagger}(B_{00})^{-1}B_{01}^{s} - A_{01}^{s}(A_{00})^{-1}A_{01}^{s\dagger}, \tag{7a}$$

$$A_{00} \to A_{00} - A_{01}^{\dagger}(A_{00})^{-1}A_{01} - A_{01}(A_{00})^{-1}A_{01}^{\dagger}, \tag{7b}$$

$$B_{00} \to B_{00} - B_{01}^{\dagger}(B_{00})^{-1}B_{01} - B_{01}(B_{00})^{-1}B_{01}^{\dagger}, \tag{7c}$$

$$A_{01} \to A_{01}(A_{00})^{-1}A_{01}, \tag{7d}$$

$$A_{01}^{\dagger} \to A_{01}^{\dagger}(A_{00})^{-1}A_{01}^{\dagger}, \tag{7e}$$

$$B_{01} \to B_{01}(B_{00})^{-1}B_{01}, \tag{7f}$$

$$B_{01}^{\dagger} \to B_{01}^{\dagger}(B_{00})^{-1}B_{01}^{\dagger}, \tag{7g}$$

$$A_{01}^{s} \to A_{01}^{s}(A_{00})^{-1}A_{01}, \tag{7h}$$

$$A_{01}^{s\dagger} \to A_{01}^{\dagger}(A_{00})^{-1}A_{01}^{s\dagger}, \tag{7i}$$

$$B_{01}^{s} \to B_{01}(B_{00})^{-1}B_{01}^{s}, \tag{7j}$$

$$B^{s\dagger}_{01} \rightarrow B^{s\dagger}_{01}(B_{00})^{-1}B^{\dagger}_{01}. \tag{7k}$$

Carrying out a sufficiently large number of iteration steps the effective interaction between principal layers will become considerably small regarding the strength of the intralayer interaction. Thus, the block matrices of the Green's function will be given in the limit of an infinitely large number of iterations by

$$(I_{00})^{-1} \rightarrow G_{00}, \tag{8a}$$

$$(A_{00})^{-1} \rightarrow G_{\mathrm{A}}, \tag{8b}$$

$$(B_{00})^{-1} \rightarrow G_{\mathrm{B}}. \tag{8c}$$

G_{00} represents the diagonal block of the Green's function of the interface principal layer. The diagonal block of the bulk Green's function is given by G_{A} for material A. The respective Green's function of material B reads G_{B}.

Setting B^{s}_{01} and $B^{s\dagger}_{01}$ from the beginning equal to zero, *i. e.* decoupling the material B region from the interface, one arrives at the renormalization instruction for a reconstructed surface of material A. In this case the interface layer plays the role of a reconstructed or relaxed layer.

2.3 Transfer matrices

As in the case of a semi-infinite solid the remaining blocks of the Green's function are accessible by means of transfer matrices. The latter are easily determined in a similar way as the renormalization instructions. We define

$$T_{\mathrm{A}} = \breve{G}_{\mathrm{A}00}A^{\dagger}_{01}, \tag{9a}$$

$$T^{\dagger}_{\mathrm{A}} = A_{01}\breve{G}_{\mathrm{A}00}, \tag{9b}$$

$$T^{s}_{\mathrm{A}} = \breve{G}_{\mathrm{A}00}A^{s\dagger}_{01}, \tag{9c}$$

$$T^{s\dagger}_{\mathrm{A}} = A^{s}_{01}\breve{G}_{\mathrm{A}00}, \tag{9d}$$

$$T_{\mathrm{B}} = \breve{G}_{\mathrm{B}00}B_{01}, \tag{9e}$$

$$T^{\dagger}_{\mathrm{B}} = B^{\dagger}_{01}\breve{G}_{\mathrm{B}00}, \tag{9f}$$

$$T^{s}_{\mathrm{B}} = \breve{G}_{\mathrm{B}00}B^{s}_{01}. \tag{9g}$$

$$T^{s\dagger}_{\mathrm{B}} = B^{s\dagger}_{01}\breve{G}_{\mathrm{B}00}, \tag{9h}$$

with the Green's function for the ideal surface of material A, $\breve{G}_{\mathrm{A}00}$, the inverse of which can be determined by the renormalization instruction

$$A_{00} \to A_{00} - A_{01}(A_{00})^{-1} A_{01}^{\dagger}. \tag{10}$$

For material B we arrive at

$$B_{00} \to B_{00} - B_{01}^{\dagger}(B_{00})^{-1} B_{01} \tag{11}$$

which converges to $\breve{G}_{\mathrm{B}00}^{-1}$. Now the whole matrix of the Green's function is available by means of

$$G_{n+1,m} = T_{\mathrm{A}} G_{n,m} \quad \text{for } 1 \leq n, m \leq n \tag{12a}$$

$$G_{1m} = T_{\mathrm{A}}^{\mathrm{s}} G_{0m} \quad \text{for } m \leq 0 \tag{12b}$$

$$G_{n,m+1} = G_{n,m} T_{\mathrm{A}}^{\dagger} \quad \text{for } 1 \leq n, n \leq m \tag{12c}$$

$$G_{0,m+1} = G_{0m} T_{\mathrm{A}}^{\mathrm{s}\dagger} \quad \text{for } 0 \leq m \tag{12d}$$

$$G_{11} = \breve{G}_{\mathrm{A}00} + T_{\mathrm{A}}^{\mathrm{s}} G_{00} T_{\mathrm{A}}^{\mathrm{s}\dagger}, \tag{12e}$$

$$G_{n+1,n+1} = \breve{G}_{\mathrm{A}00} + T_{\mathrm{A}} G_{nn} T_{\mathrm{A}}^{\dagger}, \quad \text{for } n \geq 1 \tag{12f}$$

and the similar equations for material B,

$$G_{n-1,m} = T_{\mathrm{B}} G_{n,m} \quad \text{for } n \leq -1, n \leq m \tag{13a}$$

$$G_{-1,m} = T_{\mathrm{B}}^{\mathrm{s}} G_{0m} \quad \text{for } 0 \leq m \tag{13b}$$

$$G_{n,m-1} = G_{n,m} T_{\mathrm{B}}^{\dagger} \quad \text{for } n \leq -1, m \leq n \tag{13c}$$

$$G_{0,m-1} = G_{0m} T_{\mathrm{B}}^{\mathrm{s}\dagger} \quad \text{for } m \leq 0 \tag{13d}$$

$$G_{-1-1} = \breve{G}_{\mathrm{B}00} + T_{\mathrm{B}}^{\mathrm{s}} G_{00} T_{\mathrm{B}}^{\mathrm{s}\dagger}, \tag{13e}$$

$$G_{n-1,n-1} = \breve{G}_{\mathrm{B}00} + T_{\mathrm{B}} G_{nn} T_{\mathrm{B}}^{\dagger}, \quad \text{for } n \leq -1. \tag{13f}$$

The layer-resolved density of states may be defined as

$$N_m(E) = -\frac{1}{\pi} \lim_{\eta \to 0^+} \mathrm{Im}\ \mathrm{tr}\ (S \cdot G(E + i\eta))\,|_m \tag{14}$$

where the trace is restricted to the specified principal layer m. In the same way a symmetry-resolved or orbital-resolved DOS may be introduced.

2.4 Break conditions

Because it is not possible to carry out an infinitely large number of iterations of the renormalization loop, one has to look for well-defined break conditions. For example, for the recursion method a lot of break conditions exist (Haydock 1980). In principle, the error due to the termination can be made arbitrarily small.

The simplest break condition is a definite number of iterations which has the disadvantage that in band gaps the number of iterations will be too large, whereas at band edges it may be too small, thus leading to an unknown error in the LDOS.

Therefore, consider the maximum of all matrix norms of the interlayer interaction matrices after the i-th renormalization step,

$$M_i = \max\left(\| A^{\mathrm{s}}_{01} \|, \ldots, \| B^{\mathrm{s}\dagger}_{01} \|\right). \tag{15}$$

M_0 refers to the initial interaction matrices. In the limit $i \to \infty$, M_i will vanish. We define the absolute error as M_i itself and the relative error by M_i/M_0. The iteration loop has to stop if the absolute or the relative error are below a given small value. This procedure results in a more accurate LDOS than the simple maximum iteration count break condition. For example, in the case of an onedimensional solid, in band gaps typically no more than 3 iterations are necessary to arrive at a relative error (refering to the LDOS) smaller than 0.01, whereas at band edges the number of iterations increases up to 11. In practice, the termination of the loop due to the relative error gives best results.

2.5 Averaged tight-binding parameters

Incommensurate stacking of layers cannot be treated by calculation schemes which require translational invariance parallel to the atomic layers. Therefore, we introduce averaged tight-binding parameters which take into account the variation of the interatomic distance.

In order to calculate the elements of the overlap matrix S between two incommensurable layers it is a first approximation to confine the summation to the nearest neighbour (NN) terms, which in the case of Sb/GaAs reduce to one:

$$S_{q\beta p\alpha}(\vec{k}_{\|}) = \frac{1}{N_{\|}} \sum_{j=1}^{N_{\|}} \sum_{h\in \mathrm{NN}} \exp[i\vec{k}_{\|} \cdot (\vec{R}^{\|}_{jp} - \vec{R}^{\|}_{hq})] \langle \alpha, 0|\beta, \vec{R}^{\|}_{jp} - \vec{R}^{\|}_{hq}\rangle \tag{16}$$

where $N_{\|}$ is the number of planar unit cells, jp is the index of the atomic orbital α in the j-th unit cell of the p-th layer. The Bloch sum $| \, p\alpha\rangle$ belongs to material A, whereas $| \, q\beta\rangle$ belongs to the incommensurate layer of the interface I. Using atomic wave functions (Clementi and Roetti 1974) overlap integrals can be evaluated for each atomic distance. Therefore, assumptions on a scaling with distance, such as the d^{-2} power law, are not necessary.

The sum above cannot be simplified, since all unit cells are different because of incommensurability. The directions of the vectors $\vec{R}^{||}_{jp} - \vec{R}^{||}_{hq}$ are isotropically distributed and for all (j, h) there exist index pairs (i, k), such that $\mid (\vec{R}^{||}_{jp} - \vec{R}^{||}_{hq}) - (\vec{R}^{||}_{ip} - \vec{R}^{||}_{kq}) \mid$ is arbitrarily small, *i. e.*, the vectors constitute a dense set. These facts enable the transition from summation to integration, the introduction of plane polar coordinates (r, ϕ) and a further approximation of this integral by a sum:

$$S_{q\beta p\alpha}(\vec{k}_{||}) = \frac{1}{\Omega} \sum_{j=1}^{M} \mid \vec{r}_j \mid \exp(i\vec{k}_{||}\vec{r}_j) \langle \alpha, 0 | \beta, \vec{r}_j{}^{||} \rangle \Delta r_j \Delta \phi_j. \tag{17}$$

Ω denotes the integration area $\pi r^2_{\max}$ with $r_{\max}$ being the third–next neighbour distance of the ideal GaAs crystal. In our calculations for Sb/GaAs we have chosen $M = 100$ integration points distributed on concentric circles, $\Delta\phi_j = \Delta\phi$ and $\Delta r_j = \Delta r$.

A similar calculation can be carried out for the Hamiltonian matrix elements. In the case of the calculations for the Sb/GaAs interface presented below, this is not necessary because we apply the Extended Hückel theory (EHT) which gives a direct connection between the overlap matrix elements to those of the Hamiltonian.

3 Application to Sb/GaAs

Serving as an example the electronic structure of the interface Sb/GaAs(110) has been examined. The unit cell of the semimetal Sb is rhombohedral and contains two atoms. This crystal structure is composed of two interpenetrating, trigonally distorted, face-centered-cubic lattices. The lattice constants of the hexagonal system are $a = 4.3007$Å and $c = 11.222$Å (Falicov *et al* 1966). The semiconductor GaAs cristallizes in the zincblende structure with a lattice constant of $a = 5.65325$Å (see for example Blakemore 1982). Therefore, GaAs(110) shows to be incommensurate with any of the Sb planes within a reasonable number of unit cells. There is experimental evidence, that one monolayer of Sb continues the GaAs lattice with relaxation. For coverages greater than 1ML, experimental investigations show a threedimensional island growth atop the initial Sb monolayer without long-range order (Hu *et al* 1990), *i. e.* the second Sb layer can be seen as commensurate with misfit defects or as incommensurate depending on the lateral size of the islands. Both situations have to be considered in estimating the electronic structure.

Before analysing the interface-band structure we give a sketch of the underlying theoretical assumptions of the calculation.

The knowledge of the tight-binding overlap matrix, which can be easily calculated analytically for every interatomic distance, allows the parametrization of the one-particle Hamiltonian using the Extended Hückel theory (Hoffmann 1963 and Nishida 1981):

$$H_{\alpha l\alpha l}(\vec{k}) = \widetilde{I}_{\alpha} - K_{\alpha\alpha} I_{\alpha} (S_{\alpha l\alpha l}(\vec{k}) - 1) \tag{18a}$$

$$H_{\alpha l\beta m}(\vec{k}) = -\frac{1}{2} K_{\alpha\beta} (I_{\alpha} + I_{\beta})\ S_{\alpha l\beta m}(\vec{k}) \tag{18b}$$

for $(\alpha l) \neq (\beta m)$, where α and l run over all orbital symmetries and over all basis atoms, respectively. The parameters $K_{\alpha\beta}$, I_{α} and $\widetilde{I}_{\alpha}$ are chosen to give the best fit to experimental angle-resolved photoemission data (Mårtensson *et al* 1986, Carstensen 1991) and to more sophisticated theoretical band-structure calculations (see for example Chelikowsky and Cohen 1976, Cardona *et al* 1988).

Our parameter set for GaAs has been determined by fitting to the well established bandstructure calculations of Chelikowsky and Cohen (1976) and Cardona *et al* (1988). Furthermore, we have carried out self-consistent calculations leading to nearly the same parameter set (Kruse 1990). The charge transfer from Ga to As is in good agreement with ionicity, which corroborates the use of appropriate wave functions.

Though Sb is a group V semi-metal, very suitable EHT-parameters were obtained from a fit to the bulk-band structures presented by Falicov *et al* (1966) and Bullett (1975). Our basis set consists of the $4s$- and the $4p$-orbitals of both Ga and As, as well as the $5s$- and $5p$-orbitals of Sb.

This parametrization scheme has proven its suitability in surface electronic structure and also photoemission calculations for III-V and II-VI semiconductor compounds (Henk *et al* 1993b and references therein). By considering matrix elements the latter includes also the wavefunctions, additionally showing this procedure to be physically unique, though a pure mathematical bandstructure fit alone may be not.

The (110) surface of GaAs covered with Sb requires three EHT-parameter sets. Two sets are obtained from bulk GaAs as well as from bulk Sb parametrizations. In order to determine the third set which handles the GaAs-Sb interaction, the well-established electronic structure of the system GaAs(110)-p(1×1)-Sb(1ML) (Bertoni *et al* 1983, Mailhiot *et al* 1985) has been interpolated. From our point of view this procedure results in more reliable EHT parameters than the usual arithmetic mean between the two bulk EHT parameter sets. The energies of the surface states are lying within the energy ranges given by the differences between the calculations of Bertoni *et al* (1983) and Mailhiot *et al* (1985). Furthermore, the number of surface states agrees with that in the two former calculations. This gives further support to the EHT-parametrizations for zinc-blende semiconductor compounds (Henk and Schattke 1989).

The knowledge of these Extended-Hückel parameters allows to calculate the electronic structure of systems with any number of Sb layers on any surface of the GaAs crystal supposed the atomic geometry has been determined. Because of the lack of experimental data for systems with more than one monolayer Sb, total-energy minimization calculations should be carried out. They have been done along the tight-binding formalism given by Chadi (1979). This formalism is numerically quite simple and is appropriate as long as ab initio calculations are lacking. However, for more than one layer of Sb adsorbed on GaAs(110), the incommensurability of the bulk GaAs and of the Sb crystal structures has to be considered. It globally results in lattice faults and textures, and therefore the exact atomic positions are of minor importance. In order to overcome this problem, the incommensurability is treated by applying averaged tight-binding parameters (confer subsection 2.5). The idea behind this assumption claims that sufficiently large areas of unperturbed interface structure exist to yield a unique electronic picture, as measured by angle-resolved photoemission. These areas separate incommensurable lattice regions which are taken to be of the respective bulk geometry. Systems with Sb-layers commensurate with the GaAs substrate are denoted by their specification following the substrate specification, whereas systems with incommensurate Sb-layers are denoted with their specification in front of the substrate specification. For example, the semi-infinite solid (1ML)Sb/GaAs(110)-p(1×1)-Sb(1ML) consists of the GaAs(110) substrate, on which a commensurate monolayer of Sb is adsorbed, followed by an incommensurate Sb monolayer.

Figure 1 shows the surface electronic structure of the system GaAs(110)-p(1×1)-Sb(1ML) in comparison with that of the system (1ML)Sb/GaAs(110). Though the former configuration, Sb in positions of the GaAs bulk, does not represent the established physical picture of a one-overlayer reconstruction, it has been included for convenience of comparison. It shows a surface-band structure similar to that of the uncovered GaAs(110) surface (Henk *et al* 1993b), namely surface states in the heteropolar gap, resonances at the 'stomach gap' and surface states at the valence band maximum (VBM) with a similar dispersion as the dangling-bond surface state on GaAs(110). The surface-band structure of (1ML)Sb/GaAs(110) already shows the typical features of all those systems with ideal (xML)Sb, namely a cumulation of p-type surface states within the fundamental gap of GaAs(110). Note the missing of resonances near the 'stomach gap'. Furthermore, in the heteropolar gap two surface states composed of Sb-s orbitals occur.

The next step is the analysis of systems with two layers of Sb adsorbed on the (110) surface of GaAs. The surface electronic structure has been calculated for three systems: GaAs(110)-p(1×1)-Sb(2ML) with the atomic structure being determined by total energy minimization, (2ML)Sb/GaAs(110) with an application of the averaged tight-binding parameters, and (1ML)Sb/GaAs(110)-p(1×1)-Sb(1ML) containing as surface one ideal Sb-layer also treated within the averaged tight-binding scheme.

The atomic geometry of GaAs(110)-p(1×1)-Sb(2ML) has been determined by total-energy minimization based on the assumption, that the Sb atoms of the outermost layer are placed at sites such that the twodimensional unit cell of the outermost Sb-layer is rectangular and has a two-point basis. Besides, the relaxation of the GaAs layers and the inner Sb layer is supposed to remain unchanged when the second layer Sb is adsorbed. This procedure seems to be justified, because we are interested in the general character of this system, subtle changes due to subsurface relaxations may be taken into account if experimental data are available. We used the same total energy minimization scheme as Mailhiot *et al* (1985) who determined structural parameters for both GaAs(110) and GaAs(110)-p(1×1)-Sb(1ML) which are in good correspondence with experimental data.

The following data represent the obtained differences from the positions in an ideal GaAs(110) zincblende lattice: $\Delta\vec{r}_{\rm As} = (-0.09555,\ -0.2454,\ 0.9872)$ Å, $\Delta\vec{r}_{\rm Ga} = (-0.0613,\ 0.4206,\ 1.2061)$ Å. The x-, y- and z-axes point into the directions $[1\bar{1}0]$, [001], and [110], respectively. The relaxation of the outermost Sb-layer is very strong compared to that of the inner Sb-layer. The tilt angle reads 6° and is slightly larger than that of (1ML)Sb/GaAs(110) with 3°, whereas clean GaAs(110) shows a tilt angle of 31° (Duke *et al* 1983). The mirror-plane symmetry has been destroyed by the relaxation in $[1\bar{1}0]$-direction, a first hint for effects due to incommensurability.

Figures 2a and 2b represent the resulting surface electronic structure of GaAs(110)-p(1×1)-Sb(2ML) which is rather different from that of the remaining two calculated overlayer systems, (2ML)Sb/GaAs(110) and (1ML)Sb/GaAs(110)-p(1×1)-Sb(1ML). The four surface bands running between −10.5 eV and −7.5 eV localized at the two Sb-layers are s-like in orbital character. The energy range from −7.5 eV to −6.5 eV contains surface states localized at the outermost Sb-layer which are $p_x p_y$-like, the p_x- and the p_y- orbitals being parallel to the crystal surface. Above −2 eV there are very dipersive states localized at the four outermost layers which are p_z-like in character, the p_z-orbitals aligned to the surface normal. The surface states not explicitly mentioned yet are mainly p-like in orbital character and show no pronounced localization neither at the surface nor at the interface. The crystal surface is expected to be metallic because one of the dispersive states, p_z-like in character, crosses the Fermi level (0.84 eV above VBM of GaAs) several times. Most of the surface states and resonances can be easily followed throughout the whole surface Brillouin zone (SBZ) but at certain values of $k_{||}$ some states only show an enhanced LDOS at the surface.

It could be expected that the electronic bands lying in gaps of the projected bulk-band structures of both Sb and GaAs(110) (shaded area in fig. 2a and 2b) will be observed at the GaAs-Sb interface in systems with more than two layers of Sb. Especially the variety of states in the GaAs 'stomach gap' which is not covered by the projected Sb structure seems to fulfil this assumption. To clear this point higher Sb-coverages were investigated. In contrast to the first guess the existence of interface states in the 'stomach gap' could not be confirmed, however, they were found only in the fundamental gap of GaAs(110), especially for the systems (3ML)Sb/GaAs(110) and the Sb/GaAs(110) interface (confer fig. 3), being p-like in orbital character. The system (3ML)Sb/GaAs(110) shows many surface states nearly uniformly localized at the three Sb layers. The positions and the dispersion of these states are similar to those of the systems (1ML)Sb/GaAs(110) and (2ML)Sb/GaAs(110) (cf. figure 1). Additionally and in contrast to (xML)Sb/GaAs(110), $x = 1, 2$, the (3ML)Sb/GaAs(110) system posesses interface states localized at the outermost GaAs-layer. Only these are depicted in the lower panel of fig. 3.

The missing of interface states in the 'stomach gap' can be seen by the following reasoning. In the commensurate one- and two-layer coverage these states are localized in the topmost layer which still reflects the GaAs-structure and thus show only a GaAs property. Whereas in the incommensurate case, independent of the number of layers, the assumed Sb bulk structure seems to prevent surface states in this energy regime.

There are three types of interface states: *(i)* The energy of the first type lies within bulk-band gaps of both materials, A and B. These states decay into both directions normal to the interface plane and correspond in character to the usual surface states. *(ii)* The second type of interface states possesses an energy which lies in a band gap of one material, say A, but lies in the projected bulk-band regime of the other (B) and, hence, may be resonant with the bulk states of material B. *(iii)* The third type corresponds to type two but with material A and B interchanged.

The interface electronic structure of the system terminated by a semi-infinite Sb crystal (upper panel in fig. 3) differs significantly from that of (3ML)Sb/GaAs(110). This system shows interface states localized either at the GaAs-layer or at the Sb-layer adjacent to the interface. Serving as an example, figure 4 gives the LDOS at $\overline{M}$.

Most of the interface states are lying in the fundamental gap of the projected bulk-band structure of GaAs(110). These states are of type two because their energies lie in the gap of GaAs(110) but in the projected bulk-band regime of Sb. Only two of these states show an enhanced LDOS at the GaAs layer. Furthermore, we observe two GaAs-derived states at high binding energies which correspond to the surface states found on clean GaAs(110). At -9.8 eV an As-s-like state is closely located at a bulk-band edge. This state corresponds to the A_2 state of GaAs(110). Here, we use the commonly accepted nomenclature of GaAs(110) surface states. A surface state similar to C_2 found at GaAs(110) occurs at -7.0 eV. Note the strong confinement of the interface states especially at the fundamental gap. For example, Sb-derived states induce only little LDOS in the GaAs layers, and vice versa. This may be typical for semiconductor-metal interfaces: for the Co/Cu interface one finds interface states which penetrate into up to four layers adjacent to the interface (Reiser 1993).

Because the interface electronic structures of the systems (3ML)Sb/GaAs(110) and Sb/GaAs(110) differ considerably we conclude that the boundary conditions at the surface side, *i. e.* in direction towards the Sb bulk, show effect on the interface states. To analyse the question how many Sb layers are necessary to result in an interface-band structure very close to that presented here, one has to compute the LDOS for (xML)Sb/GaAs(110) for x larger than 3. But this procedure ends in large basis sets and, therefore, in a large amount of computer time, which is not required in the interface calculation presented here. Besides other calculation schemes (see for example Skriver and Rosengaard 1992 or Crampin 1993) this renormalization procedure has obviously shown its applicability for this type of problems.

4 Conclusion

We have derived a renormalization scheme which allows the fast computation of the Green's function of interfaces. To treat incommensurate systems so-called averaged tight-binding parameters have been introduced. As a first application we have studied the interface electronic structure of Sb/GaAs(110) and compared the results with those of the GaAs(110) surface covered with up to three monolayers of Sb. Interface states are found in systems with more than two Sb-layers. Their energies lie in the fundamental band gap of GaAs, and they are strongly located at the interface layers. The system Sb/GaAs(110) shows interface states in the first Sb-layer, which are not present in (3ML)Sb/GaAs(110). Therefore, three layers of Sb are not sufficient to separate the Sb surface from the interface layer. Effects due to incommensurate adsorption are found for the states with energies in the 'stomach gap' of GaAs(110). For the systems with one or two commensurate adlayers, states in the respective energy- and $k_{||}$-regime are present, whereas they are missing in the incommmensurate systems. Because some of the interface states are clearly lying in the band gaps of the projected bulk-band structure of both Sb and GaAs, they should be detectable in angle-resolved (inverse) photoemission experiments, with not too high adsorbate coverage.

Acknowledgements

We would like to thank D. Reiser, Duisburg university, for valuable discussions and testing the renormalization computer subroutines. The numerical computations have been performed at the Regionales Rechenzentrum der Universität Köln within project P047 and the Rechenzentrum der Universität Kiel. This work is financially supported by the Bundesministerium für Forschung und Technologie, contract no. 055PGABB and 055FKTAB, and by a grant of the Land Schleswig-Holstein.

References

Ballentine L E and Kolář M 1986 *J. Phys. C: Solid State Physics* **19** 981

Bertoni C M, Calandra C, Manghi F and Molinari E 1983 *Phys. Rev. B* **27** 1251

Blakemore J S 1982 *J. Appl. Phys.* **53** R124

Bullett D W 1975 *Solid State Commun.* **17** 965

Cardona M, Christensen N E and Fasol G 1988 *Phys. Rev. B* **38** 1806

Carstensen H 1991 *thesis* Universität Kiel

Chadi D J 1979 *Phys. Rev. B* **19** 2074

Chelikowsky J R and Cohen M L 1976 *Phys. Rev. B* **14** 556

Chen A-B, Lai-Hsu Y-M and Chen W 1989 *Phys. Rev. B* **39** 923

Chen X M, Canter K F, Duke C B, Paton A, Lessor D L and Ford W K 1993 *Phys. Rev. B* **48** 2400

Clementi E and Roetti C 1974 *Atomic Data and Nuclear Data Tables* **14** 235

Crampin S 1993 *J. Phys.: Condens. Matter* **5** 4647

Duke C B, Paton A, Ford W K, Kahn A and Carelli J 1982 *Phys. Rev. B* **26** 803

Duke C B, Richardson S L, Paton A and Kahn A 1983 *Surf. Sci.* **127** 134

Falicov L M and Lin P J 1966 *Phys. Rev.* **140A** 562

Graft R D, Lohrmann D J, Pastori Parravicini G and Resca L 1987 *Phys. Rev. B* **36** 4782

Grosso G, Moroni S and Pastori Parravicini G 1989 *Physica Scripta* **T25** 316

Haydock R 1980 "The Recursive Solution of the Schrödinger Equation" *Solid State Physics* Vol. 35 (Academic Press, New York)

Henk J and Schattke W 1989 *Solid State Commun.* **70** 683

——— 1993a *Computer Physics Communications* **77** 69

Henk J, Schattke W, Carstensen H, Manzke R and Skibowski M 1993b *Phys. Rev. B* **47** 2251

Hoffmann R 1963 *J. Chem. Phys.* **39** 1397

Hu Y, Jost M B, Wagener T J and Weaver J H 1990 *Phys. Rev. B* **42** 7050

Hybertsen M S and Louie S G 1987 *Phys. Rev. Letters* **58** 1551

Kress C, Fiedler M and Bechstedt F 1993 *Physica B* **185** 400

Kruse C 1990 *diploma thesis* Universität Kiel

Lambrecht W R L and Andersen O K 1986 *Surf. Sci.* **178** 256

Lopéz Sancho M P, Lopéz Sancho J M and Rubio J 1985 *J. Phys. F: Metal Physics* **15** 851

Mårtensson P, Hansson G V, Lähdeniemi M, Magnusson K O, Wiklund S and Nicholls J M 1986 *Phys. Rev. B* **33** 7399

MacLaren J M, Crampin S, Vvedensky D D and Pendry J B 1989 *Phys. Rev. B* **40** 12164

Mailhiot C, Duke C B and Chadi D J 1985 *Phys. Rev. B* **31** 2213

Mönch W 1986 *Festkörperprobleme* **XXVI** 67

Muñoz M C, Velasco V R and Garcia-Moliner F 1987 *Physica Scripta* **35** 504

Nishida M 1981 *J. Phys. C* **14** 535

Reiser D 1993 *diploma thesis* Universität Duisburg

Rosengaard N M and Skriver H L 1993 *Phys. Rev. B* **47** 12865

Schulman J N and Chang Y-C 1983 *Phys. Rev. B* **27** 2346

Skriver H L and Rosengaard N M 1991 *Phys. Rev. B* **43** 9538

Wachutka G, Fleszar A, Máca F and Scheffler M 1992 *J. Phys.: Condens. Matter* **4** 2831

Fig. 1: Surface electronic structures of incommensurate (1ML)Sb/GaAs(110) (circles) and GaAs(110)-p(1×1)-(1ML)Sb (solid lines) along the high-symmetry lines of the surface Brillouin zone of GaAs(110). The shaded area represents the projected bulk-band structure of GaAs. Only surface states which are strongly localized in the Sb-layer are shown.

Fig. 2a: Surface electronic structure of GaAs(110)-p(1×1)-(2ML)Sb. The shaded area represents the projected bulk-band structures of GaAs(110). Only surface states which are strongly localized in the Sb-layers are shown.

Fig. 2b: See fig. 2a, but with projected bulk-band structure of Sb.

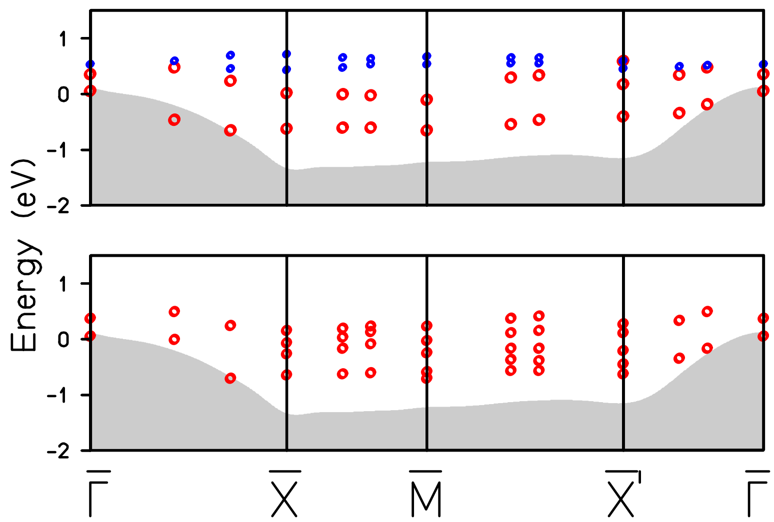

Fig. 3: Interface states of incommensurate (3ML)Sb/GaAs(110) (lower panel) and of semi-infinite Sb/GaAs(110) (upper panel). The shaded area represents the projected bulk-band structure of GaAs(110). For (3ML)Sb/GaAs(110) only states localized at the outermost GaAs-layer are shown, whereas in the upper panel GaAs-located (◯) and Sb-located (∘) are given.

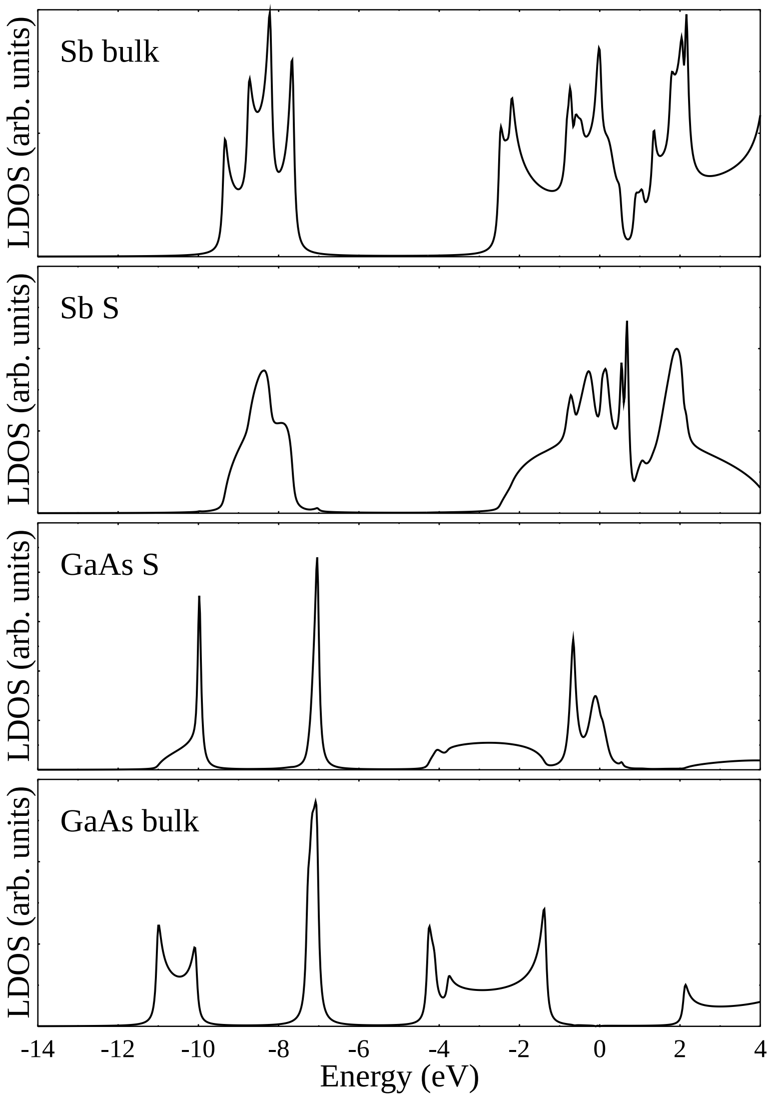

Fig. 4: Layer-resolved density of states for $\vec{k}_{||}$ at $\overline{M}$ for semi-infinite Sb/GaAs(110). The layer type is given at the left at each curve, the respective zero corresponds to the value at its left egde. All curves share a common LDOS scale and, thus, relative peak heights can be compared.